Journal of Luminescence 135 (2013) 323–326

Contents lists available at SciVerse ScienceDirect

Journal of Luminescence

journal homepage: www.elsevier.com/locate/jlumin

Hybrid white organic light-emitting devices based on phosphorescent iridium–benzotriazole orange–red and fluorescent blue emitters

Zhen-Yuan Xia [a,*], Jian-Hua Su [a], Chi-Sheng Chang [b], Chin H. Chen [b]

[a] Key Laboratory for Advanced Materials and Institute of Fine Chemicals, East China University of Science and Technology, Shanghai 200237, China
[b] Display Institute, Microelectronics and Information Systems Research Center, National Chiao Tung University, Hsinchu, Taiwan 300, China

ARTICLE INFO

Article history:
Received 2 July 2012
Received in revised form
26 August 2012
Accepted 13 September 2012
Available online 24 September 2012

Keywords:
Benzotriazole–iridium complex
Hybrid
White OLED

ABSTRACT

We demonstrate that high color purity or efficiency hybrid white organic light-emitting devices (OLEDs) can be generated by integrating a phosphorescent orange–red emitter, bis[4-(2H-benzotriazol-2-yl)-*N*,*N*-diphenyl-aniline-N^1,C^3] iridium acetylacetonate, Ir(TBT)$_2$(acac) with fluorescent blue emitters in two different emissive layers. The device based on deep blue fluorescent material diphenyl-[4-(2-[1,1′;4′,1″]terphenyl-4-yl-vinyl)-phenyl]-amine BpSAB and Ir(TBT)$_2$(acac) shows pure white color with the Commission Internationale de L'Eclairage (CIE) coordinates of (0.33,0.30). When using sky-blue fluorescent dopant *N*,*N*′-(4,4′-(1*E*,1′*E*)-2,2′-(1,4-phenylene)bis(ethene-2,1-diyl)bis(4,1-phenylene))-bis(2-ethyl-6-methyl-*N*-phenylaniline) (BUBD-1) and orange–red phosphor with a color-tuning phosphorescent material *fac-tris*(2-phenylpyridine) iridium (Ir(ppy)$_3$), it exhibits peak luminance yield and power efficiency of 17.4 cd/A and 10.7 lm/W, respectively with yellow-white color and CIE color rendering index (CRI) value of 73.

1. Introduction

White organic light-emitting diodes (white OLEDs) have attracted much attention in recent years, owing to their potential use of backlight system in full color displays and solid-state lightings with low-cost and large-area alternatives [1]. White fluorescent OLEDs can be generated by many approaches such as using vertical red–green–blue (RGB) small-molecular organic emitters stacked with different layers comprising three primary colors or two complementary colors [2–6], polymers combining R, G, B dopants in a single layer [7], utilization of broad exciplex or excimer emission [8,9], and the application of microcavity [10]. However, many of these devices suffered from poor color purity and low power efficiency.

The efficiency of OLEDs can be greatly improved by incorporating a phosphorescent dopant in an appropriate host material as the emitting layer, because it captures the triplet state energy which is lost in conventional fluorescent OLEDs. As robust deep blue phosphorescence material is still not available, most high-efficiency white OLEDs are based on the combination of blue fluorescence and orange/red phosphorescence emitter in a single device architecture, which have been called hybrid white OLEDs [11–13].

Lately, we reported an orange–red emitting iridium (III) complex based on benzotriazole–iridium derivative bis[4-(2*H*-benzotriazol-2-yl)-*N*,*N*-diphenylaniline-N^1,C^3]iridium acetylacetonate ([Ir(TBT)$_2$(acac)]) [14], which can be used as an efficient dopant in monochromatic orange–red OLEDs. The low driving voltage and high efficiency properties make this material a good candidate for the application in hybrid white OLEDs.

In this work, we integrated this orange–red phosphor with two fluorescent blue emitters as the emissive layers. High color purity or efficiency hybrid white OLEDs were achieved in the two type devices **A** and **B1**. Device **A** based on deep blue fluorescent material BpSAB and Ir(TBT)$_2$(acac) shows pure white color with the CIE coordinates of (0.33,0.30) at 10 mA/cm^2. However, the maximum luminance yield of device **A** is only 4.8 cd/A. While using the sky blue fluorescent dye BUBD-1 and co-doping a green phosphorescent Ir(ppy)$_3$ into orange–red phosphor Ir(TBT)$_2$(acac) layer, device **B1** exhibits greatly improved luminance yield of 17.4 cd/A with a red-shifted color (CIE$_{x,y}$: 0.47, 0.45).

2. Experimental details

The chemical structures of key materials and the device configuration of monochromatic PHOLED are shown in Fig. 1. The synthesis and characterization of Ir(TBT)$_2$(acac) have been published elsewhere [14,15]. Other materials were obtained commercially and used without further purification.

* Corresponding author. Tel./fax: +86 21 64252288.
E-mail address: xiazhenyuan@hotmail.com (Z.-Y. Xia).

0022-2313/$ - see front matter Crown Copyright © 2012 Published by Elsevier B.V. All rights reserved.
http://dx.doi.org/10.1016/j.jlumin.2012.09.017

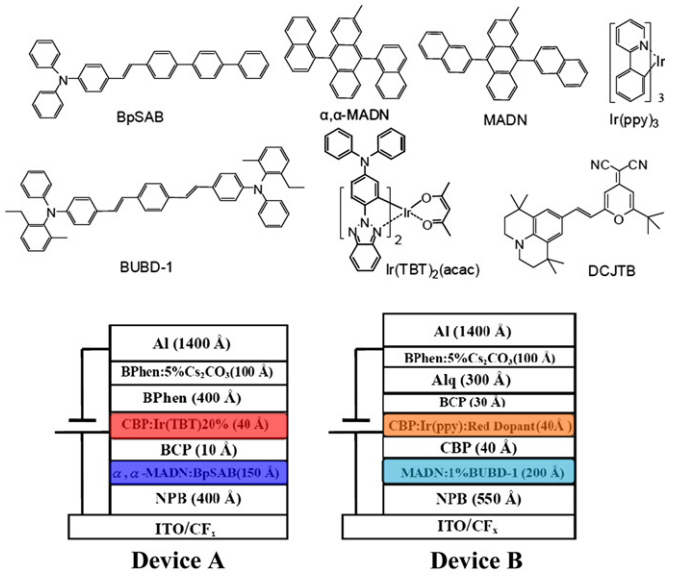

Fig. 1. Chemical structures of key materials and the configuration of two hybrid white OLEDs (devices **A** and **B**).

Prior to the deposition of organic materials, indium–tin-oxide (ITO)/glass was cleaned with a routine cleaning procedure and pretreated with oxygen plasma. Devices were fabricated under about 10^{-4} Pa base vacuum in a thin-film evaporation coater following a routine protocol. The current–voltage–luminance characteristics were measured with a diode array rapid scan system using a Photo Research PR650 spectrophotometer and a computer-controlled, programmable, direct-current (DC) source.

3. Results and discussion

According to our previous investigation, the optimized doping concentration of $Ir(TBT)_2(acac)$ is 20 wt% in single emitting layer devices. A two-element WOLED was fabricated with the device structure **A**: ITO/CF_x/NPB (400 Å)/α,α-MADN:3% BpSAB (150 Å)/BCP(10 Å)/CBP:20% $Ir(TBT)_2(acac)$ (40 Å)/Bphen(400 Å)/Bphen:Cs_2CO_3(100 Å)/Al(1400 Å) as shown in Fig. 1 (ITO = indium tin oxide, NPB = 4,4-bis[*N*-(1-naphthyl)-*N*-phenyl amino]biphenyl, Bphen = 4,7-diphenyl-1,10-phenanthroline, α,α-MADN = 2-methyl-9,10-di(1-naphthyl)anthracene, BpSAB = diphenyl-[4-(2-[1,1′;4′,1″]terphenyl-4-yl-vinyl)-phenyl]-amine, CBP = 4,4′-*N*,*N*′-di(carbazolyl)-biphenyl, and BCP = 2,9-dimethyl-4,7-diphenyl-1,10-phenanthroline). CF_x acts as the hole injection layer, NPB is the hole-transporting layer (HTL), CBP:$Ir(TBT)_2(acac)$ is the orange–red emissive layer, BPhen is the electron transporting and hole blocking layer (ETL/HBL), BPhen:Cs_2CO_3 is the *n*-doping layer, BCP is the exciton blocking layer, which prevents the triplet excitons of phosphorescent dopants being quenched by fluorescent non-radiative energy transfer, α,α–MADN is the host for deep blue dopant BpSAB, and the optimal doping concentration is ~3% [16].

The electroluminescence spectra of device **A** at different current densities are shown in Fig. 2. Two blue emission peaks at 456 nm and 476 nm are from the fluorescent dopant BpSAB and the orange–red peak at 588 nm comes from the phosphorescent dye. The relative intensity of blue emission increased slightly under low current densities (from 0.5 mA/cm^2 to 10 mA/cm^2). At high current density, the intensity of the blue peaks was about 50% higher than that of the normalized orange–red one. The color shift could be attributed to the hole blocking effect of BCP insertion layer. In device **A**, there is a large energy barrier (~0.6 eV) of hole injection from α,α-MADN host (HOMO: −5.8 eV) to BCP (HOMO: −6.4 eV) layer. Apparently large amount hole carriers are accumulated around α,α-MADN/BCP border at high driving voltage; then more excitons are generated around α,α-MADN host layer for increasing blue fluorescent emission. It is worth mentioning that the CIE value (0.33,0.30) is

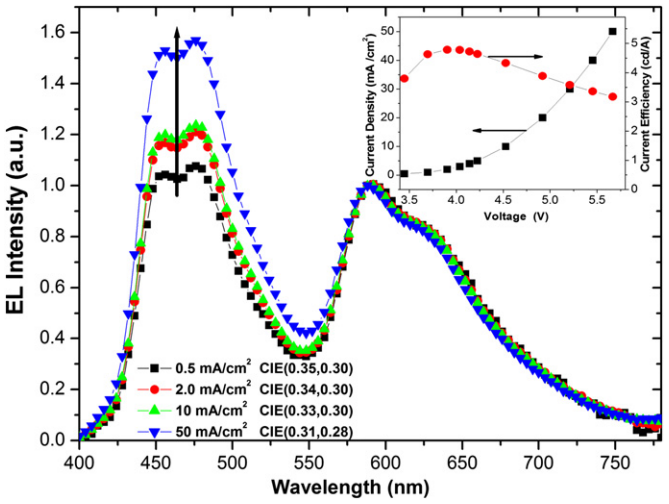

Fig. 2. EL spectra of device **A** (normalization on orange–red peak) at various current densities. Inset: the current density–voltage (*J*–*V*) and current efficiency characteristics of device **A**.

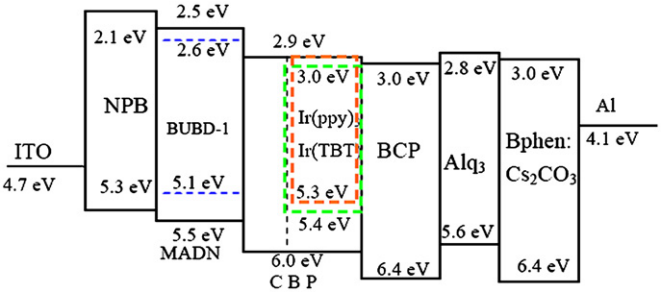

Fig. 3. Energy level diagram and the structure of device **B1**.

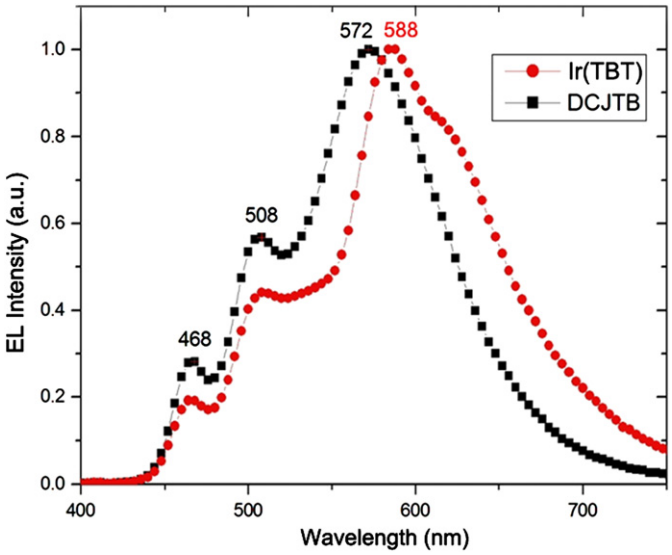

Fig. 4. Normalized EL spectra of devices **B1** and **B2** (DCJTB as the orange–red dopant) at the current density of 10 mA/cm^2.

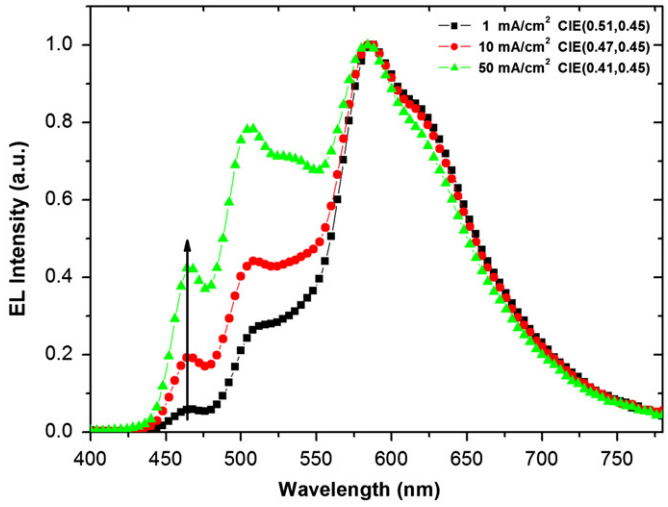

Fig. 5. Normalized EL spectra of device **B1** at various current densities.

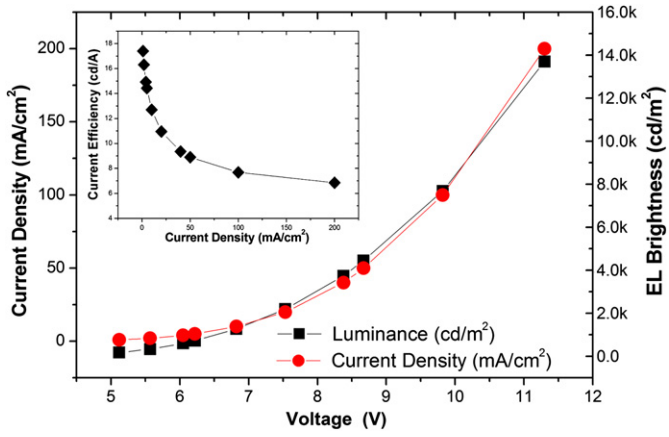

Fig. 6. Current density–voltage–luminance characteristics (*J*–*V*–*L*) of device **B1**. Inset: the current efficiency characteristics of device **B1**.

of a relativly pure white color compared with the ideal CIE coordinates (0.33,0.33) (in Figs. 2 and 7). The CIE coordinates present a negligible bluish change (0.31,0.28), while the driving current density was increased to 50 mA/cm^2 at 5.7 V. The luminance yield and external quantum efficiency (EQE) reach about 4.8 cd/A and 2.9% respectively under a current density of 2 mA/cm^2 and 3.8 V (in Fig. 2, inset). This result indicates good color stability and low driving voltage properties of device **A**. But the efficiency of device **A** is relatively poor, due to the low quantum efficiency of deep blue emitter and energetically mismatched BCP interlayer.

To further improve the luminance efficiency, we chose sky blue dopant BUBD-1 with bipolar MADN host [17] instead of deep blue one and co-doped a color-tuning phosphor Ir(ppy)$_3$ [18] in the orange–red emitting layer. An un-doped CBP interlayer plays a similar role as the BCP layer in device **A**, and it also facilitates the holes transport. The device **B1** structure was ITO/CF$_x$/NPB(550 Å)/MADN:1%BUBD-1(200 Å)/CBP(40 Å)/CBP: 8%Ir(ppy)$_3$: 4% Ir(TBT)(40 Å)/BCP(30 Å)/Alq$_3$(300 Å)/Bphen:5% Cs_2CO_3 (100 Å)/Al(1400 Å) (BUBD-1 = *N*,*N*′-(4,4′-(1*E*,1′*E*)-2,2′-(1,4-phenylene)bis(ethene-2,1-diyl)bis(4,1-phenylene))bis(2-ethyl-6-methyl-*N*-phenylaniline), Ir(ppy)$_3$ = *fac*-*tris*(2-phenylpyridine) iridium, Alq$_3$ = tris(8-hydroxyquinolinato)-aluminum) (in Fig. 3). The inserted Alq$_3$ layer between the hole blocking BCP and the *n*-doping layers helps the injection and transport of electrons. A standard device **B2** with a fluorescent dye DCJTB (4-(dicyanomethylene)-2-tert-butyl-6-(1,1′,7,7′-tetramethyljulolidin-4-yl-vinyl)-4H-pyran) 1.2% replaced the orange–red phosphor and no change of other layers was made as well.

As shown in Fig. 4, the blue fluorescent emitter (BUBD-1, 468 nm) and green/red emitter (CBP:Ir(ppy)$_3$ (508 nm):Ir(TBT) region, (588 nm)) form a broadband white light emission, and the blue/green color emission peaks are not distinct compare with the orange–red emisson peak, which leads to the reddish-white CIE position (0.47,0.45) at 10 mA/cm^2 (in Fig. 5). When the orange–red dopant material was replaced by DCJTB in device **B2** (emission peak at 572 nm), a similar spectrum is detected as well. Moreover, apparent voltage dependent variation in emission color index is observed in the EL spectra of device **B1** (in Fig. 5). With the increase of the voltage from 5.1 V (1 mA/cm^2) to 8.7 V (50 mA/

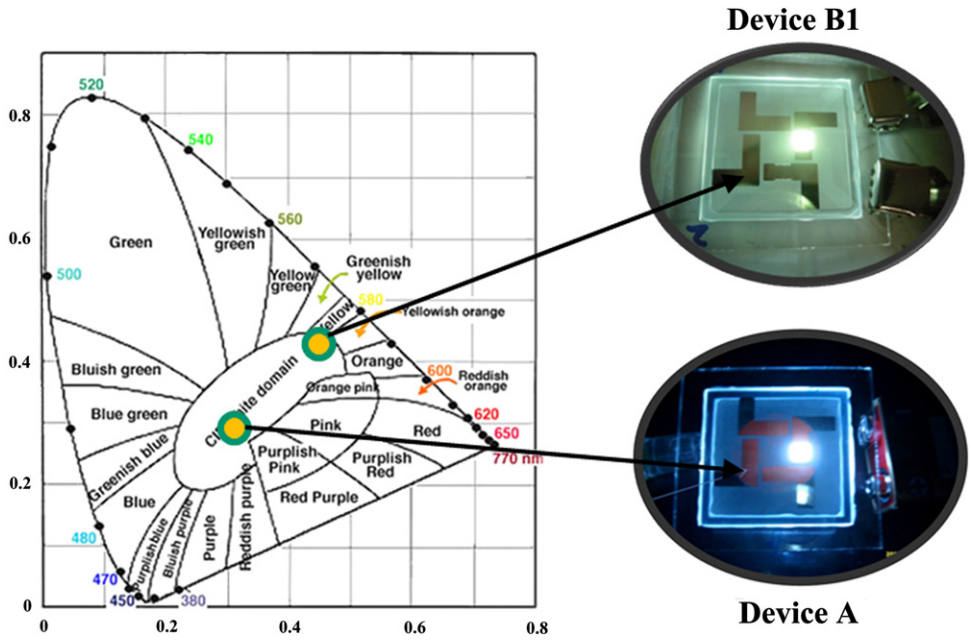

Fig. 7. CIE coordinates of devices **A** and **B1** and the photographs of their light emissions.

Table 1
Performance parameters of devices **A**, **B1** and **B2** at the current density of 10 mA/cm^2.

Device	Orange–red dopant	Voltage (V)	Current efficiency (cd/A)	Power efficiency (lm/W)	Luminance (nit)	EQE (%)	CIE 1931	CRI
A	**Ir(TBT) 20%**	**4.5**	**4.3**	**3.0**	**433**	**2.7**	**(0.33,0.30)**	**–**
B1	**Ir(TBT) 4.0%**	**6.8**	**12.7**	**5.8**	**1266**	**5.8**	**(0.47,0.45)**	**73**
B2	**DCJTB 1.2%**	**6.3**	**16.7**	**8.3**	**1665**	**6.0**	**(0.41,0.47)**	**63**

cm^2), the intensity of the blue and green emission gradually enhances relative to the red one. The weak blue emission at low current density may be explained by the unbalanced exciton recombination zone. Unlike device **A**, devices **B1** and **B2** have holes as dominated carriers due to the intrinsic property of hole-preferred CBP transporter [11]. Also, the low-lying LUMO level of CBP interlayer (LUMO: −2.9 eV) hinders electron injection into the blue host MADN (LUMO: −2.5 eV) [19], as shown in the energy level diagram of Fig. 3. Therefore, less excitons are generated at the MADN matrix and the blue BUBD-1 emission decreases. On the other side, an efficient T–T energy transfer from Ir(ppy)$_3$ to Ir(TBT)$_2$(acac) in the co-doped phosphor layer greatly reduces the green emission and enhances the orange–red one. While at higher current densities, more electrons are injected into the blue layer and the more balanced electron–hole pairs result in the enhanced blue emission. Meanwhile, the easier formation of high-energy excitons at high electric field causes enhanced green emission and better CIE value (0.41,0.45) [20]. However, the efficiency of device **B1** is seriously quenched at high drive current density (in the inset of Fig. 6); this phenomenon is also observed in the Ir(TBT)$_2$(acac) based single-emitter device [15] and device **A**. We suppose that it is due to the combination of triplet–triplet phosphorescence annihilation [21] and field-induced exciton dissociation effects [22].

The performance of our device **B1** is comparable with that of DCJTB-doped device **B2** at the current density of 10 mA/cm^2 (in Table 1), and it owns a good color rendering index (CRI) value 73. Device **B1** exhibits peak luminance and power efficiency of 17.4 cd/A and 10.7 lm/W (at 1 mA/cm^2), respectively, with a maximum luminance of 13715 cd/m^2 (at 200 mA/cm^2, in Fig. 6), which is much more improved than those of the two-element hybrid WOLED device **A**.

4. Conclusion

In summary, an orange–red iridium–benzotriazole phosphor Ir(TBT)$_2$(acac) was used in hybrid white OLEDs. Two emissive layers WOLEDs by adjusting Ir(TBT)$_2$(acac) with its complementary color (deep blue) or the other primary colors (green/blue) were fabricated. Near pure CIE value (0.33,0.30) and power consumption white OLEDs were achieved by Ir(TBT)$_2$(acac) and deep blue fluorescent emitter BpSAB. While using sky blue fluorescent dye BUBD-1, green phosphor Ir(ppy)$_3$ and Ir(TBT)$_2$(acac), the maximum luminance yield and efficiency are 17.4 cd/A and 10.7 lm/W, respectively, with good CRI value of 73.

Acknowledgements

This work is financially supported by NSFC/China (50673025, 20603009), National Basic Research 973 Program (2006CB806200) and a JD research grant of Industry/Academia Cooperation Project provided by e-Ray Optoelectronics Technology Co., Ltd. Taiwan.

References

[1] B.W. D'Andrade, S.R. Forrest, Adv. Mater. 16 (2004) 1585.
[2] P. Chen, L. Zhao, Y. Duan, Y. Zhao, W.F. Xie, G.H. Xie, S.Y. Liu, L.Y. Zhang, B. Li, J. Lumin. 131 (2011) 2144.
[3] J.H. Seo, G.Y. Kim, J.R. Koo, G.W. Hyung, K.H. Lee, J.H. Kim, S.S. Yong, Y.K. Kim, Jpn. J. Appl. Phys. 48 (2009) 052104.
[4] Y. Sun, N.C. Giebink, H. Kanno, B. Ma, M.E. Thompson, S.R. Forrest, Nature 440 (2006) 908.
[5] C.L. Ho, L.C. Chi, W.Y. Hung, W.J. Chen, Y.C. Lin, H. Wu, E. Mondal, G.J. Zhou, K.T. Wong, W.Y. Wong, J. Mater. Chem. 22 (2012) 215.
[6] L. Duan, D.Q. Zhang, K.W. Wu, X.Q. Huang, L.D. Wang, Y. Qiu, Adv. Funct. Mater. 21 (2011) 3540.
[7] Y. Liu, M. Nishiura, Y. Wang, Z.M. Hou, J. Am. Chem. Soc. 128 (2006) 5592.
[8] S.H. Kim, S.H. Park, J.E. Kwon, S.Y. Park, Adv. Funct. Mater. 21 (2011) 644.
[9] J. Feng, F. Li, W.B. Gao, S.Y. Liu, Y. Liu, Y. Wang, Appl. Phys. Lett. 78 (2001) 3947.
[10] Q. Wang, Y.T. Tao, X.F. Qiao, J.S. Chen, D.G. Ma, C.L. Yang, J.G. Qin, Adv. Funct. Mater. 21 (2011) 1681.
[11] P. Chen, W.F. Xie, J. Li, T. Guan, Y. Duan, Y. Zhao, S.Y. Liu, C.S. Ma, L.Y. Zhang, B. Li, Appl. Phys. Lett. 91 (2007) 023505.
[12] G. Schwartz, K. Fehse, M. Pfeiffer, K. Walzer, K. Leo, Appl. Phys. Lett. 89 (2006) 083509.
[13] C.L. Ho, M.F. Lin, W.Y. Wong, W.K. Wong, C.H. Chen, Appl. Phys. Lett. 92 (2008) 083301.
[14] Z.W. Xu, J. Tang, Q. Zhang, H. Tian, Chin. J. Lumin. 29 (2008) 578.
[15] Z.Y. Xia, X. Xiao, J.H. Su, C.S. Chang, C.H. Chen, D.L. Li, H. Tian, Synth. Met. 159 (2009) 1782.
[16] M.H. Ho, Y.S. Wu, S.W. Wen, M.T. Lee, T.M. Chen, C.H. Chen, K.C. Kwok, S.K. So, K.T. Yeung, Y.K. Cheng, Z.Q. Gao, Appl. Phys. Lett. 89 (2006) 252903.
[17] M.F. Lin, L. Wang, W.K. Wong, K.W. Cheah, H.L. Tam, M.T. Lee, C.H. Chen, Appl. Phys. Lett. 89 (2006) 121913.
[18] B.W. D'Andrade, M.A. Baldo, C. Adachi, J. Brooks, M.E. Thompson, S.R. Forrest, Appl. Phys. Lett. 79 (2001) 1045.
[19] D.S. Qin, Y. Tao, Appl. Phys. Lett. 86 (2005) 113507.
[20] H.I. Baek, C.H. Lee, J. Phys. D 41 (2008) 105101.
[21] S. Reineke, K. Walzer, K. Leo, Phys. Rev. B 75 (2007) 125328.
[22] J. Kalinowski, W. Stampor, J. Mezyk, M. Cocchi, D. Virgili, V. Fattori, P. Di Marco, Phys. Rev. B 66 (2002) 235321.